Ferromagnetic order-disorder transition in an Ising fluid

M. J. P. Nijmeijer,[1] A. Parola,[2] and L. Reatto[1]
[1]*INFM and Dipartimento di Fisica, Università degli Studi di Milano, via Celoria 16, 20133 Milano, Italy*
[2]*INFM and Istituto di Scienze Fisiche, Università degli Studi di Milano, via Lucini 3, Como, Italy*
(Received 1 July 1997)

The Ising fluid we have investigated is a system of hard spheres which carry an Ising spin. A short range ferromagnetic potential acts between particles. A renormalization group study of the model, based on the hierarchical reference theory of fluids, gives quantitative predictions on the phase diagram and the phase boundaries. The model can show two distinct phase transitions: a magnetic order-disorder transition and a liquid-vapor phase separation which meet at a tricritical point. The critical properties of the magnetic transition have been studied by Monte Carlo simulations at two densities in systems with up to 4000 particles. The locations of the critical points are in good agreement with the theoretical estimates. However, a finite-size scaling analysis shows effective critical exponents which deviate from the expected Ising values. These discrepancies resemble the analogous result of a previous numerical study of Heisenberg fluids. Here they are interpreted as due to crossover phenomena, partly related to Fisher exponent renormalization induced by the presence of noncritical density fluctuations. [S1063-651X(97)09012-0]

PACS number(s): 61.20.−p, 64.60.Fr

I. INTRODUCTION

Models of fluids made of particles with some internal degree of freedom like a spin are of current theoretical interest [1]. Phase transitions of different character can take place in such systems, as studies of the phase diagram and of the associated critical phenomena have shown. In particular, recent simulations studied the magnetic transition in the Heisenberg fluid [2]. This is a classical fluid in which all particles carry a Heisenberg spin. Two particles interact via an exchangelike potential. In addition they have a hard core which prevents them from overlapping. Such a fluid displays, besides transitions between a solid, a liquid, and a vapor phase, a magnetic order-disorder transition. The simulations studied the critical properties of this transition in the fluid region, away from the liquid-vapor phase boundary. A finite-size scaling analysis gave critical exponents that are different from those for the lattice Heisenberg model. Also, the obtained critical fourth-order cumulant is different from the value for the lattice.

These results differ from what is expected theoretically and are not well understood. They could be ascribed to the use of too-small systems in the simulations, prohibiting the observation of the correct critical exponents. However, the presence of such ''corrections to scaling'' is rendered less plausible by the fact that the same exponents are obtained for the three fluid densities which were studied. Moreover, the critical indices satisfy an exact exponent relation and the critical cumulants show no trend towards the value for the lattice when the system size is increased. They do, however, show a slight dependence on the fluid's density [2].

A possible theoretical picture of the magnetic phase transition is that of ''Fisher renormalization'' [3]. It relates the critical exponents of the fluid to the exponents of the corresponding lattice model. For example, the exponents for the Ising fluid are expressed in terms of those for the Ising lattice model. Fisher renormalization predicts that in the canonical ensemble (in which the simulations were carried out) the critical exponents of the fluid and the lattice are the same if the lattice specific heat exponent α_l is negative. If, on the other hand, the lattice specific heat diverges ($\alpha_l>0$), the exponents for the fluid are expected to be ''renormalized'' in the following way. The fluid specific heat exponent becomes $\alpha=-\alpha_l/(1-\alpha_l)$, the magnetization exponent β becomes $\beta=\beta_l/(1-\alpha_l)$ (with β_l the lattice exponent), the susceptibility exponent γ becomes $\gamma=\gamma_l/(1-\alpha_l)$ (with γ_l the lattice exponent), and similarly for the correlation length exponent $\nu=\nu_l/(1-\alpha_l)$.

The lattice specific heat exponent appeared to be well established by three successive simulations [4–6]: $\alpha_l=-0.144(9)$. This value is also in reasonable agreement with series expansions and transfer matrix studies (see the references in [5,6]). It would imply that the lattice and the fluid exponents are the same. However, the most recently published simulation of the Heisenberg lattice [7] differs sharply from previous results and gives $\alpha_l=0.075(2)$. Hence the sign of α_l remains in doubt although we consider the dissonant result as questionable.

There are no such diverging views on the lattice Ising model in three dimensions. Monte Carlo (MC) simulations, Monte Carlo renormalization group, transfer matrix, and ϵ-expansion studies (see [8,9], and references therein) give $\alpha_l>0$ ($\alpha_l=0.110(2)$ [9]). Hence, according to Fisher renormalization and insisting that $\alpha_l<0$ for the Heisenberg model, the situation for the Ising fluid should be different. The Ising fluid is defined as the Heisenberg fluid with the Heisenberg spins replaced by Ising spins. Even though the predictions of Fisher renormalization are not borne out for the Heisenberg fluid, it is worthwhile to see what happens for the Ising fluid.

An additional motivation for this study is that for the Ising fluid it is possible to study in detail the criticality and the crossover phenomena by an appropriate analytical theory [10], the hierarchical reference theory (HRT), initially devel-

oped for simple fluids and mixtures but easily applicable to the Ising fluid. HRT is a liquid-state theory which embodies the renormalization group (RG) structure close to a critical point. In HRT one studies how the free energy and the correlation functions evolve upon inclusion of fluctuations of increasing length scales, starting with the properties of a system with purely repulsive forces. With HRT one can study the universal as well as the nonuniversal quantities and the possible presence of crossover effects.

Simulations of the two-dimensional Ising fluid and its lattice gas representation exist already [11]. These simulations studied the point where the magnetic transition line touches the liquid-vapor line. The simulations found that the two lines connect in a tricritical point and measured the tricritical exponents. The study, carried out in the grand-canonical ensemble, did not address the issue of Fisher renormalization.

We carried out MC simulations of the three-dimensional Ising fluid, in close analogy with the simulations for the Heisenberg fluid [2]. We have studied by simulations only the magnetic order-disorder transition. In addition, we have studied the Ising fluid by HRT in an Ornstein-Zernike approximation and the effects of a finite cutoff in the renormalization scheme are examined. In this scheme a finite cutoff mimics the finite size of simulated systems. The model we have studied consists of particles interacting with the potential

$$\phi(\mathbf{r}_i,\mathbf{r}_j,s_i,s_j)=\begin{cases}\infty, & r_{ij}<\sigma\\ -J(r_{ij})s_is_j, & \sigma<r_{ij}<2.5\sigma\\ 0, & r_{ij}>2.5\sigma\end{cases} \quad (1)$$

where $\phi(\mathbf{r}_i,\mathbf{r}_j,s_i,s_j)$ denotes the potential between a particle i with position $\mathbf{r}_i$ and spin s_i and a particle j with position $\mathbf{r}_j$ and spin s_j. The spins can take the values 1 and -1. A hard-core repulsion at distances r_{ij} ($r_{ij}=|\mathbf{r}_i-\mathbf{r}_j|$) smaller than σ prohibits these interparticle distances while two particles further than 2.5σ away from each other do not interact. The Ising-like potential, acting at intermolecular distance r, has a ferromagnetic, Yukawa type coupling constant:

$$J(r)=\epsilon\frac{\sigma}{r}\exp\left(\frac{-r+\sigma}{\sigma}\right), \quad (2)$$

where ϵ sets the energy scale of the interaction. The coupling constant is the same as used for the Heisenberg fluid [2].

The paper is organized as follows. In Sec. II we show how the model can be studied by HRT. In Sec. III we present the method and the results of the simulations at two different densities. A final section contains a discussion of the results and our conclusions.

II. RENORMALIZATION GROUP ANALYSIS

In this section we present an analysis of the Ising fluid by renormalization group methods, in order to determine the general features of the phase diagram and the expected universality classes at the critical points. We adopt a microscopic implementation of momentum space RG, which allows for a rather accurate study of the nonuniversal properties of a model together with the exact treatment of the universal features within the ϵ-expansion framework. This method is known as hierarchical reference theory of fluids [10] and has been previously applied to simple fluids and to the Ising model. An extension of the formalism to binary mixtures was also provided showing that Fisher renormalization of the critical exponents due to field mixing [3] has to be expected at generic critical points of binary fluids when approached along a regular path in the density-concentration plane.

The HRT description of critical phenomena in binary mixtures can be directly applied to the Ising fluid problem by observing that the mapping $(\uparrow,\downarrow)\rightarrow(A,B)$ which associates an up (down) spin to an ''A'' (''B'') particle provides a correspondence between the ferromagnetic Ising fluid and a mixture of hard spheres with attractive (repulsive) interactions between like (unlike) particles. By introducing the total density of the mixture $\rho=\rho_A+\rho_B$ and the density difference $c=\rho_A-\rho_B$ we can express the magnetic properties of the Ising fluid in terms of the corresponding quantities in the mixture. In particular, the magnetization and susceptibility are related to the concentration x and the osmotic compressibility by

$$m\rightarrow c=\rho(2x-1),$$
$$\chi\rightarrow\left[\frac{1}{V}\frac{\partial^2 A}{\partial c^2}\right]^{-1}, \quad (3)$$

where A is the Helmholtz free energy. In order to get some rough information on the phase diagram to be expected, we can perform a mean field study of the model starting from the approximate representation of the free energy of the mixture:

$$-\beta A(\rho_A,\rho_B,T)=-\beta A^{ex}_{\mathrm{HS}}(\rho_A+\rho_B)+V\Big[-\rho_A\ln\rho_A\sigma^3 -\rho_B\ln\rho_B\sigma^3+\frac{\beta a}{2}(\rho_A-\rho_B)^2\Big], \quad (4)$$

where A^{ex}_{HS} is the excess Helmholtz free energy of a hard-sphere fluid at density $\rho_A+\rho_B$ and $a\sim 15.32\epsilon\sigma^3$ is the integral of the (truncated) Yukawa potential (2) which defines our model. This mean field approximation leads to the phase diagram of Fig. 1(a) where the projection of the critical lines on the density-magnetization plane is shown. Two distinct second-order transitions are visible in this approximation: a ferromagnetic critical line which extends up to high density and a liquid-vapor critical line joining the critical points of the two fully polarized states. In Fig. 1(b), the ferromagnetic critical line at zero magnetization is plotted in the density-temperature plane: This is the transition we are going to study in some detail in the following. The intersection of the two critical lines gives rise to a tricritical point which is predicted to occur at fairly low density ($\rho_t\sigma^3\sim 0.1$) within mean field approximation. Mean field theory is usually expected to give a good qualitative description of the phase diagram even if fluctuations are likely to modify the quantitative details and will certainly lead to nonclassical critical exponents. In particular, a binary mixture is believed to fall in the same universality class as simple fluids and Ising

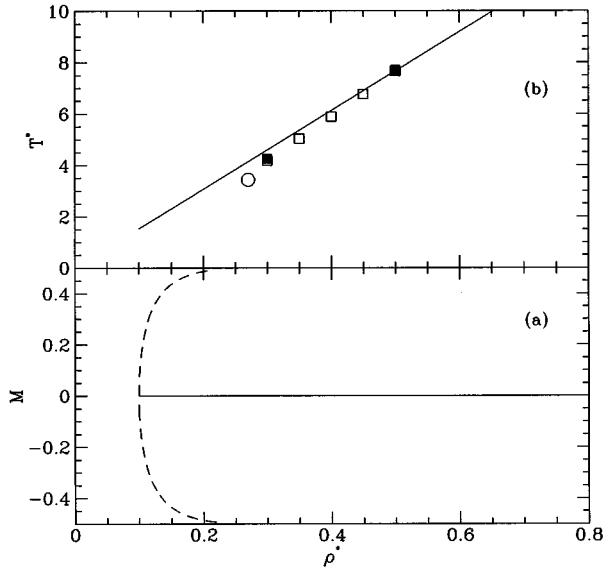

FIG. 1. Mean field critical lines of the Ising fluid projected onto in the density-magnetization plane (a). The continuous line is the magnetic transition, the dashed line is the liquid-vapor critical line. In (b) the magnetic critical line is shown in the density-temperature plane. Open squares are the estimates of HRT. The Monte Carlo values at $\rho^*=0.5$ and $\rho^*=0.3$ are represented by full squares, barely distinguishable from the HRT values. The HRT estimate of the tricritical point is marked by an open circle.

model when its physical properties are expressed as a function of *fields* (i.e., temperature and chemical potentials) rather than *densities* [12]. As noted by Fisher [3], in the density-concentration (here density-magnetization) plane, the critical exponents turn out to be *renormalized* by a factor $1/(1-\alpha_I)$ due to the nonanalytic relationship between density and chemical potential. Here α_I represents the Ising critical exponent governing the divergence of the specific heat. Such a Fisher renormalization of critical exponents is, however, hard to detect because of the generally small reduced temperature range where the power laws characterizing the critical singularity acquire the $(1-\alpha_I)$ correction [13]. Low density critical points and vicinity of critical end points have been recently identified as favorable conditions for the observability of Fisher renormalization [14]. An interesting question to be addressed is whether the Ising fluid model provides a case where signs of exponent renormalization may be detected in numerical simulations. In order to investigate this problem from the theoretical side, however, considerably more powerful tools than mean field approximations are required.

Renormalization group ideas can be directly applied to a microscopic model of binary mixture by introducing a cutoff wave vector Q for density and concentration fluctuations and deriving an exact hierarchy of equations describing the evolution of physical quantities when the momentum cutoff Q is changed. In the HRT approach this is achieved by defining a sequence of auxiliary systems characterized by cutoff dependent ferromagnetic interactions $J_Q(r)$ whose Fourier components coincide with those of the fully interacting system at wave vectors k larger than Q while vanishing identically for $k<Q$. At the limiting value $Q=\infty$ fluctuations over all length scales are suppressed thereby recovering the mean field picture, while at $Q=0$ the fully interacting model is restored. Therefore the rather artificial introduction of the cutoff wave vector Q is a mean for gradually introducing fluctuations into the model. The exact ''evolution'' equation for the fluctuation contribution $\mathcal{A}$ to the Helmholtz free energy in a d-dimensional model of mixture considerably simplifies with respect to the case of a generic mixture [10] due to the special symmetry of the Ising fluid and reads

$$-\frac{d}{dQ}\left(\frac{-\beta\mathcal{A}^Q}{V}\right)=\frac{\Omega_d}{2(2\pi)^d}Q^{d-1}\ln[1+\mathcal{F}_{cc}^Q(k)\beta J(k)], \tag{5}$$

where Ω_d is the d-dimensional solid angle, $J(k)$ is the Fourier transform of the truncated Yukawa interaction $J(r)$, Eq. (2), and $\mathcal{F}_{cc}^Q$ is the particular combination of the partial structure factors, at cutoff Q, which governs concentration fluctuations:

$$\mathcal{F}_{cc}(k)=\rho_A S_{AA}(k)+\rho_B S_{BB}(k)-2\sqrt{\rho_A\rho_B}S_{AB}(k). \tag{6}$$

This differential equation can be studied by introducing an *approximate* relationship expressing the structure factors in terms of the free energy. The closure we adopted suitably generalizes the well known random phase approximation in liquid-state theory and is conveniently expressed as an ansatz for the wave vector dependence of the direct correlation functions $\mathcal{C}_{ij}$ of the mixture, which are algebraically related to the partial structure factors by the Ornstein Zernike equation. Here, the labels (i,j) identify the type (i.e., spin) of the particles. More precisely, the closure relation we have studied is

$$\mathcal{C}_{ij}^Q(k)=c^{\mathrm{HS}}(k)+\lambda_{ij}^Q J(k), \tag{7}$$

where c^{HS} are the direct correlation function of the hard-sphere fluid and the parameters λ_{ij}^Q are defined by the requirement that our approximation (7) satisfies the exact compressibility sum rule which relates the long wavelength limit of the direct correlation functions to the second density derivatives of the free energy:

$$\mathcal{C}_{ij}^Q(k=0)=\frac{\partial^2(-\beta\mathcal{A}^Q/V)}{\partial\rho_i\partial\rho_j}. \tag{8}$$

Therefore Eq. (5) becomes a *partial* differential equation for the free energy density as a function of the cutoff Q and of the density of the two species (ρ_A,ρ_B). Such an equation has been solved numerically by an implicit finite difference scheme on a 20×20 mesh in the density-concentration plane. The ferromagnetic critical temperatures at several densities have been determined and are shown by open symbols in Fig. 1(b). We see that the HRT result is close to the mean field estimate at the higher densities while deviating near the tricritical point which we have approximately located at a density considerably higher than the mean field one: $\rho_t\sigma^3\sim0.27$, $kT_t\sim3.35\epsilon$ (in mean field $\rho_t\sigma^3\sim0.1$, $kT_t\sim1.5\epsilon$).

The occurrence of a tricritical point at the end point of the critical line is a direct consequence of the up-down symmetry of the Ising fluid model and is generally expected in this system. In Fig. 2 results from the numerical integration of

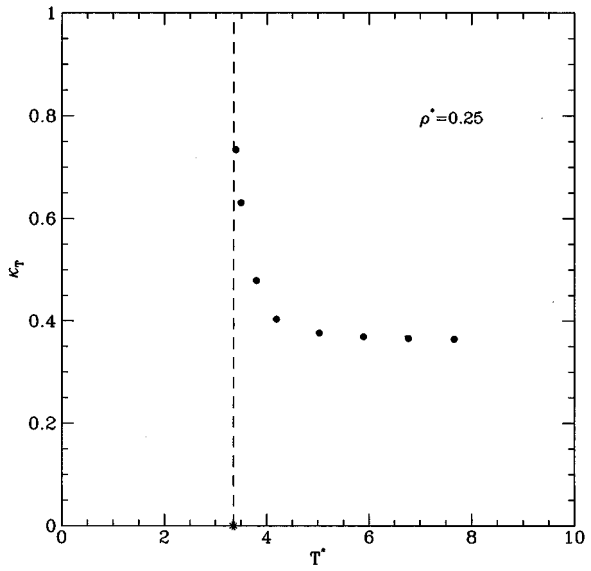

FIG. 2. Dimensionless isothermal compressibility as a function of temperature along the isochore $\rho^*=0.25$ close to the tricritical density. The dashed line shows an estimate of the tricritical temperature. Data are obtained by integration of the nonlinear HRT equations.

the HRT equation are shown along the isochore $\rho^*=\rho\sigma^3=0.25$ not far from the tricritical density. The growth of κ_T when approaching the tricritical point is apparent from the numerical data although the numerical mesh size is too small for attempting a quantitative evaluation of the corresponding tricritical exponent.

As far as the universal critical properties of the Ising fluid at a generic critical point along the ferromagnetic line, HRT does predict the phenomenon of exponent renormalization [10]. In fact, an analytical study of the exact hierarchy near dimension $d=4$ shows that the long wavelength fluctuations should be described by two scalar fields (ϕ_1,ϕ_2) which, for the Ising fluid, represent magnetization and density fluctuations. The effective action acquires the general form.

$$S[\phi_1,\phi_2]=\int d\mathbf{x}\left\{\frac{1}{2}|\nabla\phi_1|^2+H[\phi_1,\phi_2]\right\},$$

$$H[\phi_1,\phi_2]=r\phi_1^2+g^2\phi_2^2+u\phi_1^4+wg\phi_1^2\phi_2, \qquad (9)$$

which suitably generalizes the familiar ϕ^4 form of simple fluids. The four coupling constants (r,g,u,w) are nonuniversal parameters which do not affect the universality class of the model but may strongly influence the extension of the asymptotic regime and the strength of the corrections to the scaling behavior. In particular, the parameter r is the ''mass'' of the strongly fluctuating field ϕ_1 (the magnetization in our case), while u represents the self-interaction of this field, analogously to the usual, one component order parameter case. Instead g^2 is the ''mass term'' for the weakly fluctuating field (representing density fluctuations in our model). Finally, the coupling constant w is the ''mixing'' parameters which couples density and magnetization fluctuations and leads to the exponent renormalization. For instance, because of this coupling, the susceptibility diverges with an exponent $\gamma_I/(1-\alpha_I)$, slightly larger than the corresponding Ising value, when the temperature approaches its critical value. At the same time the isothermal compressibility also diverges at the ferromagnetic transition, with a small exponent $\alpha_I/(1-\alpha_I)$, the divergence being induced by the coupling between the two fluctuations. If $w=0$, no exponent renormalization is present and the isothermal compressibility remains finite. Clearly, the larger is the coupling w, the stronger are the effects of exponent renormalization. A detailed study shows that the crossover temperature $t_\times$ scales as the mixing parameter w raised to the quite large power $2/\alpha_I\sim 17$ leading to an extremely sensitive dependence of the crossover phenomenon on the value of the mixing parameter.

We have used the partial differential equation (5) to obtain estimates for these coupling constants for the Ising fluid, by stopping the HRT evolution at a cutoff wave vector $Q_0\sigma\sim 0.4$, sufficiently small that most of the short wavelength fluctuations have been included and the effective action (9) can be considered a good approximation to the exact form. The effects of the long wavelength fluctuations have been accurately studied by an examination of the effective action (9) in dimension d: The RG flow of the four parameters (r,g,u,w) has been modeled by use of a linearized form of the RG equations, correct to leading order in $\epsilon=4-d$ [10]:

$$-Q\frac{dr}{dQ}=2r+(6u-f)(1-2r),$$

$$-Q\frac{du}{dQ}=\epsilon u-(6u-f)^2,$$

$$-Q\frac{df}{dQ}=\epsilon f-f(24u-5f), \qquad (10)$$

where $f=w^2/g^2$. We have chosen to switch to these simpler RG equations, rather than to follow the full HRT evolution, mainly because this procedure allows for a very close approach to the critical point which would have been otherwise prevented by the uncertainties in the numerical integration of the partial differential equation (5). In such a way, we have been able to study the behavior of the *effective* critical exponents when the temperature closely approaches T_c. As usual, the RG flow is stopped when the momentum cutoff Q matches the physical inverse correlation length $\xi^{-1}\sim\sqrt{2r}Q$, i.e., when $2r\sim 1$. Equations (10) faithfully describe the RG flow: in particular they display both Ising and Fisher-renormalized fixed points which can be calculated analytically together with the corresponding critical exponents. Critical indices satisfy scaling relations and, in $d=3$, their values are rather close to the commonly accepted ones: $\eta=0$, $\nu_I=0.6$, $\gamma_I=1.2$, $\alpha_I=0.2$ near the Ising fixed point. The Fisher-renormalized exponents are obtained by dividing the Ising values by $(1-\alpha_I)=0.8$.

By numerically integrating these equations we can estimate the behavior of the physical quantities (free energy, compressibility, etc.) as a function on temperature. In particular, the effective critical exponents can be obtained as a function of the reduced temperature thereby providing a

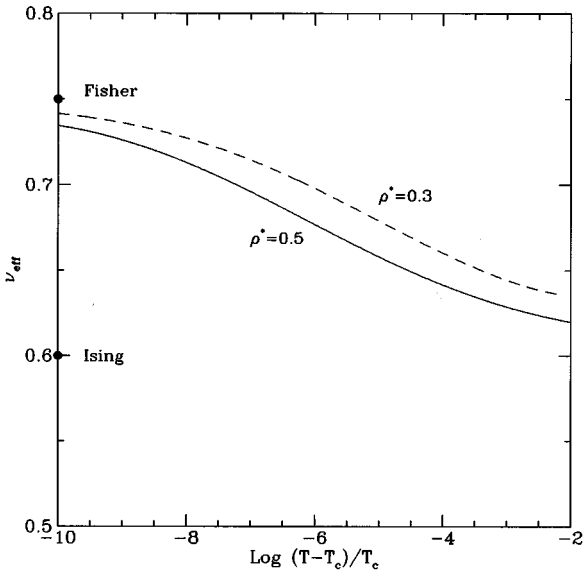

FIG. 3. Effective exponent ν for the divergence of the susceptibility as a function of the reduced temperature as predicted by HRT. The Ising and Fisher-renormalized exponents are marked on the axis. The base of the logarithms is 10.

measure of the crossover between the unstable Ising fixed point and the stable Fisher fixed point. A typical result for the exponent $\nu_{\rm eff}=-d\ln\xi/d\ln(T-Tc)$ is shown in Fig. 3 where a clear monotonic crossover between the two values corresponding to Ising ($\nu_I=0.6$) and Fisher renormalized ($\nu=0.75$) occur through several decades. Such a slow crossover can be easily interpreted as a power law divergence if experimental or numerical data are available in a limited range of reduced temperatures. Although the effects of these crossover phenomena on the critical exponents may be considered as due to the presence of strong corrections to scaling, the RG analysis shows that their origin is in fact quite different. Usual corrections to scaling are due to the contributions of irrelevant operators around a unique fixed point, and are therefore characterized by universal subleading exponents. Instead, crossovers originate from the competition of different fixed points which may attract the RG flow up to some characteristic length scale. Therefore, in general, the slow change in critical exponents determined by crossovers cannot be fitted by use of the standard methods developed in the framework of the corrections to scaling problem.

III. SIMULATIONS

Simulations of the three-dimensional Ising fluid in the canonical ensemble have been performed. The particles are enclosed in a cubic box with periodic boundary conditions.

We vary the temperature T in our simulations while keeping the density fixed. We do this for two densities: $\rho^*=0.3$ and $\rho^*=0.5$ (where $\rho^*=\rho\sigma^3$). The systems have a number of particles N ranging from $N=108$ to $N=2000$ (for $\rho^*=0.3$) or from $N=108$ to $N=4000$ (for $\rho^*=0.5$). All systems are listed in Tables I and II.

The simulations proceed in nearly the same way as those for the Heisenberg fluid. We use the Wolff algorithm [15] to update the particle spins and intertwine it with the update of the particle positions. The construction of one Wolff cluster is followed by two sweeps through the system, in each of which we try to move each particle once. The maximum displacement of the particles is such that the acceptance rate of particle displacements is around 50%. All runs consist of 10^6 sweeps with the corresponding 0.5×10^6 Wolff updates.

We carried out one run in which we performed 20 sweeps through the system between two Wolff updates. It allowed us to check that the ratio of sweeps to Wolff steps does not influence the data. The results are listed in Table III, which shows that there is indeed no such influence.

As for the Heisenberg fluid, we measure the moments of the magnetization distribution. For Ising spins, the magnetization m of a particle configuration is defined as

$$m=\frac{1}{N}\left|\sum_{i=1}^{N}s_i\right|. \tag{11}$$

During the simulations, we store the energy and the magnetization of the current configuration after each tenth Wolff update. From these data, we can calculate canonical averages of magnetization and energy moments at the temperatures at

TABLE I. Number of particles N and temperatures T of the runs carried out at the density $\rho^*=0.3$. The second and third columns are the results for the average energy $\langle u\rangle$ and the average magnetization $\langle m\rangle$ from the run.

N	T	$\langle u\rangle$	$\langle m\rangle$
108	4	−1.095(1)	0.5449(7)
108	4.3	−0.798(1)	0.4066(7)
256	4	−1.098(1)	0.5297(7)
256	4.3	−0.754(1)	0.3407(8)
500	4	−1.1080(9)	0.5283(5)
500	4.3	−0.730(1)	0.2945(8)
1000	4	−1.1153(6)	0.5289(3)
1000	4.3	−0.7138(9)	0.2509(8)
2048	4.1	−0.9746(7)	0.4421(5)
2048	4.3	−0.7019(7)	0.2092(7)

TABLE II. Number of particles N and temperatures T of the runs carried out at the density $\rho^*=0.5$. The second and third columns are the results for the average energy $\langle u\rangle$ and the average magnetization $\langle m\rangle$ from the run.

N	T	$\langle u\rangle$	$\langle m\rangle$
108	7.5	−1.329(3)	0.4642(7)
108	8.5	−0.692(2)	0.2779(6)
256	7	−1.941(2)	0.6148(4)
256	8	−0.804(2)	0.2759(6)
500	7.5	−1.234(2)	0.4155(6)
500	7.8	−0.877(2)	0.2780(7)
1000	7.6	−1.075(2)	0.3478(8)
1000	7.9	−0.757(1)	0.2012(7)
2048	7.6	−1.060(1)	0.3351(8)
2048	7.9	−0.726(1)	0.1563(6)
4000	7.6	−1.057(1)	0.3310(7)
4000	7.9	−0.7077(9)	0.1181(5)

TABLE III. Effect of the ratio of move sweeps N_s to Wolff updates N_W. The two runs are carried out at $\rho^*=0.5$, $T=7.5$ and $N=108$. Results are shown for the average energy $\langle u\rangle$, the average magnetization $\langle m\rangle$, the susceptibility χ, and the fourth-order cumulant u_4. There is no significant effect of the ratio N_s/N_W.

N_S 10^6	N_W 10^6	$\langle u\rangle$	$\langle m\rangle$	χ	u_4
5	0.25	−1.329(3)	0.465(1)	0.612(3)	0.505(1)
1	0.5	−1.329(3)	0.4642(7)	0.615(2)	0.5036(8)

which we performed the simulations. The histogram reweighting technique allows us to calculate these moments at an arbitrary temperature (not too far from the temperatures at which we performed the simulations) [16].

Error bars were obtained by dividing each run in 50 blocks. Histogram reweighting was carried out on the corresponding blocks of runs at different temperatures (but the same number of particles and density). In this way, we obtained 50 estimates of any quantity we studied at each temperature. Standard deviations were calculated from these averages.

For quantities whose average depends on the sample size (such as the susceptibility), we did not use the block results. We used results averaged over entire runs to calculate such quantities. The block results were only used to calculate error bars on these quantities.

By varying the number of blocks and its effect on the error bars, we verified that 50 was a small enough number of blocks to obtain quasi-independent block averages.

Our random number generator (RNG) was based on two binary feedback shift registers, one of length 9689, the other of length 127, which are combined by means of the exclusive-or operation. For comparison, we carried out one run with the subtract-with-carry (SWC) RNG [17,18]. This RNG is believed to be inferior to the former [19,20]. The results are shown in Table IV. The differences between the two RNG's are rather large but too small to substantiate a systematic effect of the choice of RNG.

Simulations of systems up to 1000 particles were carried out on a HP 9000 735 workstation. The systems of 2048 and 4000 particles ran at a Cray C-90.

A. Results for the density $\rho^*=0.5$

At the density $\rho^*=0.5$ we carried out simulations of systems from 108 to 4000 particles. Precise run parameters are listed in Table I together with the average energy and magnetization at those temperatures and system sizes. Figure 4 shows the Binder parameter u_4 (also called the fourth-order cumulant) [21],

$$u_4=1-\frac{\langle m^4\rangle}{3\langle m^2\rangle^2}, \tag{12}$$

where the brackets $\langle\ \rangle$ denote a canonical average, as a function of the temperature for the six system sizes. We determined the 15 intersection points and their error bars (the latter are calculated from 50 intersection points obtained from the 50 block results for each system size). We fitted [22] the intersection points (T_i, u_{4i}) of the curve for N and N' particles to the relation $T_i=T_c+c/\ln b$ with c a constant, $b=N'/N$, $N'>N$ [4,5,21]. Similarly $u_{4i}=u_{4c}+c'/\ln b$. The temperature T_c is the critical temperature, u_{4c} the critical Binder parameter.

The fit gives for $N=108$ and N' all the larger sizes (from 256 to 4000 particles): $T_c=7.722(4)$, $c=(3\pm3)10^{-3}$, and a goodness of fit $Q=0.03$ for the critical temperature (all temperatures are in units ϵ/k_B, k_B is Boltzmann's constant). For the critical Binder parameter we obtain $u_{4c}=0.453(2)$, $c'=(-4\pm11)10^{-4}$, $Q=0.38$.

Taking $N=256$ we obtain $T_c=7.726(5)$, $c=(-2\pm3)10^{-3}$, $Q=0.10$ and $u_{4c}=0.453(3)$, $c'=(1\pm2)10^{-3}$, $Q=0.45$.

Taking $N=500$ (in which case only three intersection points remain) we obtain $T_c=7.711(6)$, $c=(9\pm3)10^{-3}$, $Q=0.89$ and $u_{4c}=0.459(4)$, $c'=(-5\pm2)10^{-3}$, $Q=0.88$.

Finite-size scaling (FSS) predicts the magnetization at T_c, m_c, to vary with the linear system size L as $m_c\propto L^{-\beta/\nu}$ with β and ν the magnetization and correlation length exponents, respectively [21]. We attempted straight line fits of $\ln m_c$ versus $\ln L$ for various estimates of T_c. If we include all systems (from 108 to 4000 particles) in the fits, we obtain the best straight fits for $T_c=7.72(1)$ with, however, a poor best Q value $Q=0.03$. If we limit the fits to systems from 500 to 4000 particles we obtain $T_c=7.70(2)$ with a best Q value $Q=0.40$, see Fig. 5. With a final estimate $T_c=7.71(2)$ the straight fits to systems with a minimum size of 500 particles give $\beta/\nu=0.49(7)$.

TABLE IV. Comparison of results obtained with the subtract-with-carry (SWC) and the combined shift-register (CSR) random number generator. Both runs are carried out with $N=108$, $T=7.5$, $\rho^*=0.5$ and consist of 10^6 sweeps with 0.5×10^6 Wolff updates. The CSR data are also shown in Table III.

RNG	$\langle u\rangle$	$\langle m\rangle$	χ	u_4
SWC	−1.333(3)	0.4661(7)	0.609(2)	0.5061(7)
CSR	−1.329(3)	0.4642(7)	0.615(2)	0.5036(8)

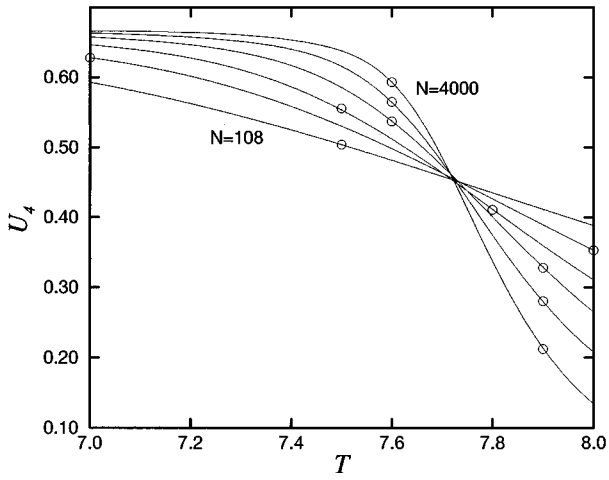

FIG. 4. Fourth-order cumulant as a function of temperature and system size for the density $\rho^*=0.5$. The circles show the results of individual simulations (error bars on these results are smaller than the symbol size), the lines result from multihistogram reweighting.

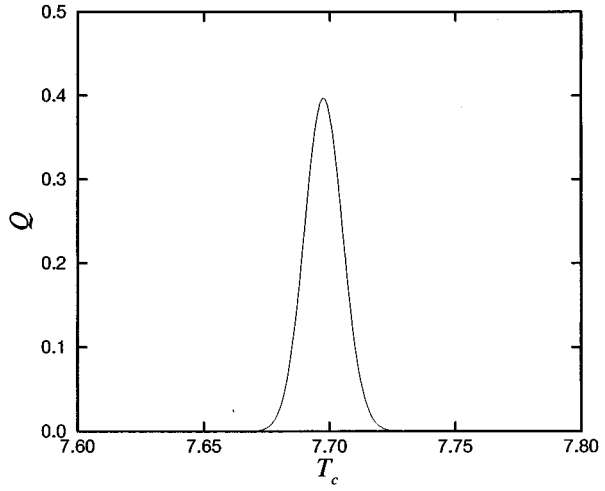

FIG. 5. Goodness of fit Q of straight-line fits of $\ln m_c$ versus $\ln L$ as a function of the estimated critical temperature T_c. The fits are for the density $\rho^*=0.5$ and exclude the system sizes $N=108$ and $N=256$.

Straight line fits of $\ln\langle m^2\rangle$ at T_c versus $\ln L$ for $T_c=7.71(2)$ give $2\beta/\nu=0.9(1)$.

The exponent ratio γ/ν with γ the susceptibility exponent has been obtained from the FSS of the susceptibility χ:

$$\chi=\frac{L^3}{k_BT}(\langle m^2\rangle-\langle m\rangle^2). \tag{13}$$

The susceptibilities as a function of the temperature are shown in Fig. 6. The maximum of the susceptibility should scale as $\chi_m\propto L^{\gamma/\nu}$ [21]. Straight line fits $\ln\chi_m=c+(\gamma/\nu)\ln L$ give $\gamma/\nu=1.906(4)$ but a poor $Q=0.08$, see Fig. 7. A closer inspection shows that this poor Q value is due to a slight scatter of the data points around the best straight line fit. For this reason, the fit does not change significantly if we limit it to the four largest system sizes: $\gamma/\nu=1.912(8)$ and $Q=0.02$.

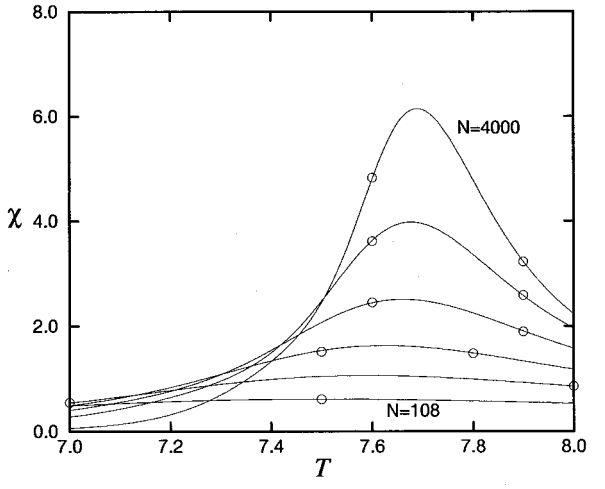

FIG. 6. Susceptibility χ as a function of the temperature and the system size for the density $\rho^*=0.5$. The circles show the results of individual simulations (error bars on these results are smaller than the symbol size), the lines result from multihistogram reweighting.

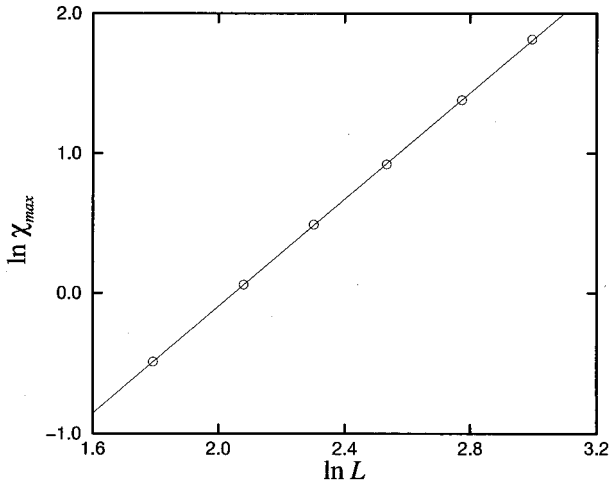

FIG. 7. Circles denote the maximum of the susceptibility χ_m as a function of the system length L on a log-log scale. Error bars are smaller than the symbol size. The line is the best straight line fit to the data. The fit is poor ($Q=0.08$) due to a slight scatter in the data, not visible on this scale.

The expected scaling of the susceptibility at T_c, χ_c, is identical. A straight line fit of $\ln\chi_c$ versus $\ln L$ yields $\gamma/\nu=1.924(4)$, $Q=0.30$ for $T_c=7.71$ and all system sizes included. Limiting the fit to the systems of 500 particles and more, we obtain $\gamma/\nu=1.930(8)$ and $Q=0.16$.

We used three estimators to determine the ratio $1/\nu$: $\partial\ln m/\partial T$, $\partial\log m^2/\partial T$, and $\partial u_4/\partial T$. All three exhibit a minimum as a function of the temperature which should diverge to $-\infty$ with the system size as $L^{1/\nu}$ [8].

A straight line fit of $\ln(\partial\ln m/\partial T)_{\min}$ versus $\ln L$ yields $1/\nu=1.573(4)$, $Q=0.01$ if all system sizes are included. The four largest systems give $1/\nu=1.55(1)$, $Q=0.28$. This strong increase of Q indicates a slight curvature in the data although the change in the slope $1/\nu$ is small.

A similar fit for $\partial\ln m^2/\partial T$ yields $1/\nu=1.562(9)$, $Q=0.35$ for the four largest system sizes. The estimator $\partial u_4/\partial T$ gives $1/\nu=1.52(2)$, $Q=0.37$.

Our final estimates are $T_c=7.71(2)$, $u_{4c}=0.456(6)$, $\beta/\nu=0.51(2)$, $\gamma/\nu=1.92(2)$, and $1/\nu=1.54(3)$ for the density $\rho^*=0.5$. They are summarized in Table V.

A striking feature in these results is the low estimate of γ/ν. The Ising lattice model has $\gamma/\nu=1.963(3)$ [9] and this ratio should not change for the fluid if the arguments of Fisher renormalization hold. We checked whether our results can be explained by corrections to FSS. We fitted the data for χ_m to the functional form $\chi_m(L)=c_1L^{\gamma/\nu}+c_2L^{-y+(\gamma/\nu)}$. All system sizes were included in the fit. The ratio γ/ν is

TABLE V. Summary of results. Our exponent ratios have been obtained without allowing for corrections to FSS. The results for the Ising lattice are taken from Blöte *et al.* [9].

ρ^*	T_c	u_{4c}	β/ν	γ/ν	$1/\nu$
0.3	4.259(5)	0.462(4)	0.54(2)	1.931(8)	1.47(4)
0.5	7.71(2)	0.456(6)	0.51(2)	1.92(2)	1.54(3)
Lattice	4.51152(2)	0.4652(3)	0.519(2)	1.963(3)	1.587(2)

fixed at 1.963 in the fit and the correction exponent y should be positive. For y in the range $y=0.2$–0.9 we obtain the fits with Q values in the range 0.12–0.19. The maximum Q values occur for $y=0.5$–0.6. For $y=0.6$ the amplitudes are $c_1=(1.60\pm0.01)10^{-2}$ and $c_2=(6.7\pm0.4)10^{-3}$. These fits are better, although not convincingly good, than the straight line fits of $\ln\chi_m$ versus $\ln L$ in which γ/ν is a fit parameter.

Equally striking is our estimate for $1/\nu$ which is in between the value 1.5887(4) for the Ising model and the value 1.409(4) which is expected from ''Fisher renormalization'' (both values are obtained from Ref. [8]). We tried to reproduce both these values by allowing for corrections to scaling. We fitted the data for the minimum of $\partial \ln m/\partial T$ to the functional form $\partial \ln m/\partial T=a_1L^{1/\nu}+a_2L^{-y+(1/\nu)}$.

With $1/\nu$ fixed at 1.5887 and all data included in the fit, we obtain very poor fits for all values of y. For example, we obtain $Q=0.01$ for $y=0.01$ decreasing to $Q=0.005$ for $y=0.5$. If on the other hand we fix $1/\nu$ at 1.409 we obtain $Q=0.24$ for $y=0.3$, decreasing to $Q=0.23$ for $y=0.2$ and $Q=0.19$ at $y=0.4$. The amplitudes are $a_1=(7.92\pm0.07)10^{-2}$ and $a_2=(-5.6\pm0.1)10^{-2}$.

However, if we limit the fit to the four largest system sizes we obtain very different results. If we fix $1/\nu$ at 1.5887 we obtain fits that become increasingly better with increasing y. For example, we obtain $Q=0.89$ for an unacceptably high value $y=2.5$. If, on the other hand, we fix $1/\nu$ at 1.409 we obtain increasingly better fits for decreasing values of y. For example, we obtain $Q=0.07$ for $y=0.3$ increasing to $Q=0.19$ for $y=0.01$.

We conclude that our data are not good enough to reliably study corrections to scaling. We extract leading-order exponents from our fits and bear in mind that they should be considered as ''effective exponents.''

B. Results for the density $\rho^*=0.3$

The analysis for $\rho^*=0.3$ is similar but does not include a system of 4000 particles. The largest system that we simulated at this density contains 2048 particles.

The fits of the intersection points of the Binder parameter yield $T_c=4.26(3)$, $c=(-5\pm3)10^{-3}$, $Q=0.75$ for the critical temperature and $u_{4c}=0.466(2)$, $c=(2\pm1)10^{-3}$, $Q=0.88$ for the critical Binder parameter. These data are for the intersection with the $N=108$ curve. The intersection with the $N=256$ curve gives $T_c=4.259(5)$, $c=(-8\pm30)10^{-4}$, $Q=0.54$ and $u_{4c}=0.462(4)$, $c=(7\pm20)10^{-4}$, $Q=0.63$.

Straight line fits of $\ln m_c$ versus $\ln L$ are good for an estimate of T_c as $T_c=4.26(1)$. The goodness of fit peaks at $Q=0.94$. The fit includes all system sizes.

With a final estimate $T_c=4.259(5)$ the fits give $\beta/\nu=0.54(2)$.

Straight line fits of $\ln\chi_m$ versus $\ln L$ give $\gamma/\nu=1.941(6)$, $Q=0.23$ if all system sizes are included in the fit. If we omit the system of 108 particles we obtain $\gamma/\nu=1.931(8)$, $Q=0.67$.

Straight line fits of the susceptibility at T_c (with $T_c=4.259$) yield $\gamma/\nu=1.942(5)$, $Q=0.19$ with all system sizes included. Discarding the smallest system we obtain $\gamma/\nu=1.932(7)$, $Q=0.68$

Our three estimators for $1/\nu$ all show a pronounced failure of the FSS scaling laws for the smallest system, see Fig. 8. It is not possible to fit all data to a straight line on a log-log scale. Therefore we omitted the $N=108$ system from our fits.

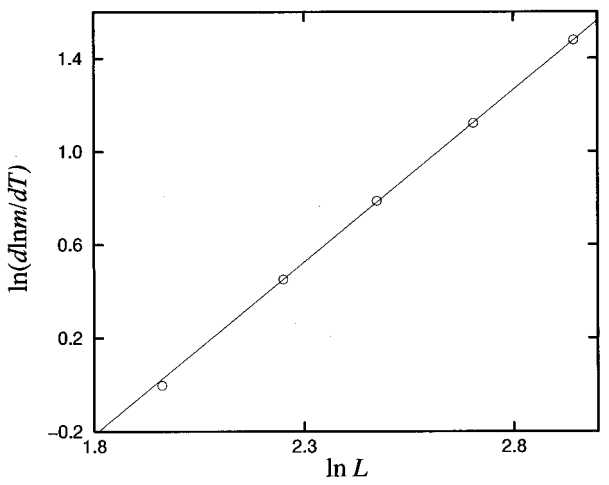

FIG. 8. Circles denote the logarithmic derivative of the magnetization m as a function of the system length L on a log-log scale. Error bars are smaller than the symbol size. The line is the best straight line fit to the data for the four largest system sizes. The smallest system size deviates visibly from the fit.

The estimator $\partial \ln m/\partial T$ yields $1/\nu=1.48(1)$, $Q=0.57$, $\partial \ln m^2/\partial T$ yields $1/\nu=1.50(1)$, $Q=0.47$, and $\partial u_4/\partial T$ yields $1/\nu=1.41(3)$, $Q=0.37$ If, for the latter estimator, we limit the fit to the three largest systems we obtain $1/\nu=1.42(6)$, $Q=0.16$.

Combining these results we finally estimate $T_c=4.259(5)$, $u_{4c}=0.462(4)$, $\beta/\nu=0.54(2)$, $\gamma/\nu=1.931(8)$, and $1/\nu=1.47(4)$ for $\rho^*=0.3$. The results are summarized in Table V.

We also inspected (for both densities) the specific heat c_V which, as a function of temperature, has a maximum. The maximum grows with increasing system size. It proved, however, difficult to distinguish between a developing divergence and a developing cusp singularity, i.e., between $\alpha_{\rm eff}>0$ and $\alpha_{\rm eff}<0$. The growth of the peak height in passing from a system of N particles to a system of roughly $2N$ particles neither accelerates nor slows down with increasing N.

IV. DISCUSSION

In comparison with the results for the Heisenberg fluid [2], the simulation data for the Ising fluid are less accurate. In particular, corrections to finite-size scaling play a larger role. This is manifested in lower Q values for many fits and the observation that different estimators of a given quantity sometimes give results that are barely consistent with each other. For example, χ_m predicts a ratio $\gamma/\nu=1.912(8)$ whereas χ_c gives $\gamma/\nu=1.930(8)$ at the density $\rho^*=0.5$. Moreover, appropriate fits that try to explain our results by leading-order Ising (or Fisher-renormalized) behavior plus a correction term sometimes work reasonably well.

Not allowing for such corrections to scaling, we obtain a set of exponents that is the same for the two densities. They satisfy the exponent relation $(2\beta+\gamma)/\nu=d$ (with $d=3$): $(2\beta+\gamma)/\nu=2.94(4)$ at $\rho^*=0.5$ and 3.01(4) at $\rho^*=0.3$. Also the critical Binder parameter is the same at the two

densities. It is not distinguishable from the value for the Ising lattice and this is also true for the ratio β/ν [8]. On the other hand, the ratio γ/ν appears to be lower than the ratio for the lattice and so does the exponent $1/\nu$.

This was different for the Heisenberg case for which the values of u_{4c} were significantly different for the lattice and the fluid. The exponents $1/\nu$ on the other hand were the same. The ratio β/ν was slightly higher in the fluid. As far as the ratio γ/ν is concerned, the situation for the Heisenberg and the Ising case is similar. In both cases one finds a value for γ/ν that is significantly lower in the fluid.

Note that our estimates of $1/\nu$ in the Ising fluid are in between those for the lattice and the value predicted by Fisher renormalization [3]: $1/\nu=(1-\alpha_I)/\nu_I=1.409(4)$. This lends support to an interpretation of our data as a crossover phenomenon.

In order to better understand the simulation results we have tried to mimic the finite-size scaling behavior by use of renormalization group equations. Clearly, we cannot directly address the issues related to the ratio γ/ν because the approximations of our RG equations (10) imply $\eta=0$ and then $\gamma/\nu=2$ at both the competing fixed points. However, we can investigate the problem of how the critical exponent ν changes when the characteristic length scale increases: RG equations can be used for getting a qualitative idea about the extent of finite-size corrections to the critical singularity, which is quite an important issue when numerical simulations are performed near a critical point. In fact, momentum space RG, and equivalently HRT, sets a cutoff Q which prevents the occurrence of long wavelength fluctuations, thereby playing a role analogous to the simulation box dimension: $L\propto 1/Q$. This interpretation gets some support from the observation that the Binder parameter u_4, which attains a nontrivial value only *at* the critical point as $L\to\infty$, can be expressed, via the correspondence $L\leftrightarrow 1/Q$, in terms of the fixed point solution of the RG equations. Therefore, up to a proportionality factor, we can identify the cutoff Q with the reciprocal of the box size and extract information about the finite-size scaling from the RG flow. In particular we have solved the approximate RG equations (10) with initial conditions appropriate for the critical point at the two densities $\rho^*=0.5$ and $\rho^*=0.3$ which have been investigated by simulation. Figure 9 shows the (reduced) temperature derivative of the inverse susceptibility as a function of the ''box size'' $L=2\pi/Q$ along the momentum cutoff integration. From scaling law arguments, this derivative should diverge in both cases as $L^{1/\nu}$ with $\nu=\nu_I/(1-\alpha_I)=0.75$ within our approximation. In fact, if the integration is carried out up to extremely large L this result is correctly recovered. However, up to boxes of $L\sim 100\sigma$ (which correspond to hundreds of thousands of particles in the simulation box) the results are different at the two densities. The lower density shows an effective exponent $\nu\sim 0.66$ which is still considerably smaller than the asymptotic one. Instead, the higher density seems still dominated by the Ising fixed point with a corresponding critical exponent ν which is only slightly larger than its Ising value $\nu_I=0.6$, within this approximation. Therefore RG analysis reproduces the same qualitative features encountered in the simulations, with strong crossovers along the whole magnetic critical line of this model. Some hint of the true asymptotic critical behavior can be found at lower densities even if the critical exponents still present slow variations over enormously large length scales, showing that in this system quantitative results cannot be extracted from simulations.

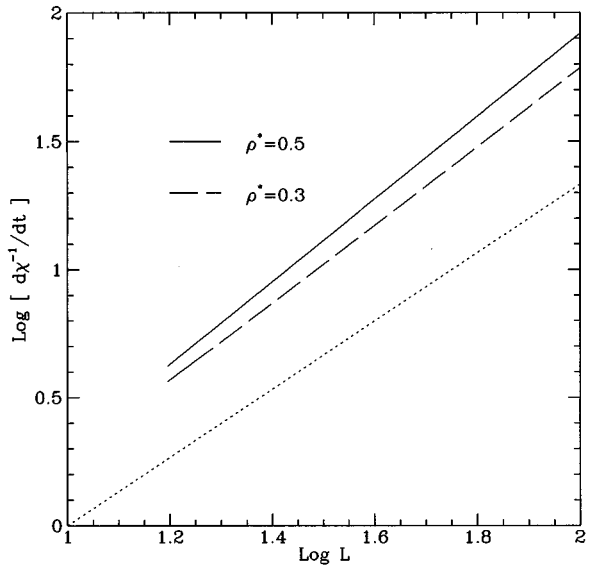

FIG. 9. Size scaling of the temperature derivative of the inverse susceptibility as mimicked by momentum space renormalization group evolution equations. The dotted line shows the expected asymptotic slope $1/\nu=4/3$. The base of the logarithms is 10.

This comparative study suggests that simulations of critical phenomena in fluids with internal degrees of freedom, or equivalently in mixtures, can be affected by strong nonuniversal crossovers which hide the true asymptotic critical behavior giving effective critical exponents with rather good power law fits slowly approaching the asymptotic value. This phenomenology is related to the presence of two competing fixed points which, in our model, correspond to Ising and Fisher renormalized critical exponents. More generally, we expect similar crossovers whenever an unstable fixed point strongly affects the RG flow over nonnegligible length scales. In these circumstances, the interpretation of experimental or simulation data on the basis of a simple power law behavior which characterizes the asymptotic region may lead to the apparent violation of scaling laws and of the universality of critical phenomena.

The model we investigated here, due to its simplicity, turns out to be particularly suitable for the study of crossover phenomena and finite-size scaling both via numerical simulations and renormalization group techniques. The same system, besides representing the simplest classical model of a fluid with internal degrees of freedom, can be fruitfully used for studying the critical phenomena associated to the presence of a tricritical point and the competition between magnetic phase transition and phase separation. We hope these problems will be addressed in future works.

ACKNOWLEDGMENT

M.J.P.N. acknowledges financial support from EEC Contract No. ERBCHBGCT940721 within the ''Human Capital and Mobility'' program.

[1] M. J. P. Nijmeijer and J. J. Weis, in *Annual Review of Computational Physics IV*, edited by D. Stauffer (World Scientific, Singapore, in press).
[2] M. J. P. Nijmeijer and J. J. Weis, Phys. Rev. Lett. **75**, 2887 (1995); Phys. Rev. E **53**, 591 (1996).
[3] M. E. Fisher, Phys. Rev. **176**, 257 (1968).
[4] P. Peczak, A. M. Ferrenberg, and D. P. Landau, Phys. Rev. B **43**, 6087 (1991).
[5] C. Holm and W. Janke, Phys. Rev. B **48**, 936 (1993).
[6] K. Chen, A. M. Ferrenberg, and D. P. Landau, Phys. Rev. B **48**, 3249 (1993).
[7] R. G. Brown and M. Ciftan, Phys. Rev. Lett. **76**, 1352 (1996).
[8] A. M. Ferrenberg and D. P. Landau, Phys. Rev. B **44**, 5081 (1991).
[9] H. W. J. Blöte, E. Luijten, and J. R. Heringa, J. Phys. A **28**, 6289 (1995).
[10] A. Parola and L. Reatto, Adv. Phys. **44**, 211 (1995).
[11] N. B. Wilding and P. Nielaba, Phys. Rev. E **53**, 926 (1996).
[12] R. B. Griffiths and J. C. Wheeler, Phys. Rev. A **2**, 1047 (1970).
[13] M. E. Fisher and P. E. Scesney, Phys. Rev. A **2**, 825 (1970).
[14] D. Pini, L. Reatto, and A. Parola, J. Phys.: Condens. Matter **9**, 1417 (1997).
[15] U. Wolff, Phys. Rev. Lett. **62**, 361 (1989).
[16] A. M. Ferrenberg and R. H. Swendsen, Phys. Rev. Lett. **63**, 1195 (1989).
[17] G. Marsaglia, B. Narasimhan, and A. Zaman, Comput. Phys. Commun. **60**, 345 (1990).
[18] A. M. Ferrenberg, D. P. Landau, and Y. J. Wong, Phys. Rev. Lett. **69**, 3382 (1992).
[19] H. W. J. Blöte and J. R. Heringa (private communication).
[20] J. R. Heringa, H. W. J. Blöte, and A. Compagner, Int. J. Mod. Phys. C **3**, 561 (1992).
[21] K. Binder, Z. Phys. B **43**, 119 (1981).
[22] W. H. Press, B. P. Flannery, S. A. Teukolsky, and W. T. Vetterling, *Numerical Recipes—The Art of Scientific Computing* (Cambridge University Press, Cambridge, England, 1986).